Distribution of homopolymer in lamellar self-assembled diblock copolymer/homopolymer blends involving specific interactions

Klymko, T.; Subbotin, A.; ten Brinke, G.

Published in:
Macromolecules

DOI:
10.1021/ma062527n

Distribution of Homopolymer in Lamellar Self-Assembled Diblock Copolymer/Homopolymer Blends Involving Specific Interactions

T. Klymko,[†] A. Subbotin,[†,‡] and G. ten Brinke*,[†]

Laboratory of Polymer Chemistry and Zernike Institute for Advanced Materials, University of Groningen, Nijenborgh 4, 9747 AG Groningen, The Netherlands, and Institute of Petrochemical Synthesis, Russian Academy of Sciences, Moscow 119991, Russia

Received November 1, 2006; Revised Manuscript Received February 16, 2007

ABSTRACT: The strongly segregated lamellar state of blends of a diblock copolymer with a "long" homopolymer that interacts favorably with one of the blocks of the copolymer is analyzed in detail. The main observations concern the parabolic homopolymer distribution profile, the presence of "dead" zones near the block copolymer interface where no homopolymer is present, and the maximal amount of homopolymer that can be dissolved. Essential parameters are the interfacial tension, the length, and composition of the block copolymer and the Flory−Huggins parameter $\chi < 0$ representing the favorable interaction between the homopolymer and one of the blocks of the copolymer. Applications are presented for blends consisting of polystyrene-*block*-poly(4-vinylpyridine) diblock copolymers and poly(2,6-dimethyl-1,4-diphenyl oxide) homopolymers. If the favorable interaction is too weak, no homopolymer will dissolve at all due to the unfavorable conformational effects accompanying an inhomogeneous homopolymer distribution.

1. Introduction

Blends of a diblock copolymer with a homopolymer that is chemically identical to one of the blocks have been studied extensively in the past both experimentally and theoretically.[1−16] In the case of a lamellar self-assembled state, it is well-known that the spatial distribution of the homopolymer depends on its relative molar mass. For low molar masses, the homopolymer will be distributed uniformly throughout the layers of the corresponding block. For a molar mass of the homopolymer that is comparable to that of the corresponding block, the homopolymer will be confined to the center of the layers, i.e., segregated in the mid-plane. A significantly higher molar mass of the homopolymer, finally, results in macrophase separation. For blends of block copolymers with homopolymers that have a specific exothermic interaction with one of the blocks of the block copolymer the situation is different. Experimentally, this situation has been investigated by different groups.[17−22] In several studies polystyrene-based block copolymers were combined with poly(2,6-dimethyl-1,4-diphenyl oxide) (PPO). Paul and co-workers[19,20] used styrene−butadiene−styrene triblock copolymers, whereas Hashimoto and co-workers[21] used styrene−isoprene diblock copolymers. In all cases an increased solubilization of PPO in the PS domains, as compared to the solubilization of homopolymer polystyrene, was observed. For the systems with PPO, the effect of the molar mass of PPO was found to be small or nonexistent, which was ascribed to the favorable interaction between PS and PPO.[23]

In our own experimental work we used PPO in combination with PS to introduce entanglements in the core of nanorods made from polystyrene-*block*-poly(4-vinylpyridine) (PS-*b*-P4VP) diblock copolymers and consisting of a PS core and a poly(4-vinylpyridine) (P4VP) corona.[24] In relation to this, the distribution of the PPO homopolymer inside the PS domains is of major interest. Theoretically, blends of a diblock copolymer with a homopolymer that interacts favorably with one of the blocks of the diblock copolymer have been addressed already, however, essentially from a stabilization point of view.[25−31] Borukhov and Leibler[25,26] discussed the enthalpic stabilization of brush-coated particles in a polymer melt and showed how favorable enthalpic interactions can change the structure of the brush from a dry brush to a wet brush. The favorable interactions can stabilize such colloidal dispersions. Of course, the essential difference between homopolymer penetration inside the grafted chains of a polymer brush compared to a block copolymer layer is the possibility of the latter to adjust the interface area per block copolymer chain. Balsara and co-workers[27,28] considered A/B/A−C blends from the perspective of stabilizing immiscible homopolymers with block copolymer surfactants for which $\chi_{AC} < 0$, the two other χ parameters being positive. Shull and co-workers[29] considered blends of an AB diblock copolymer and a A- and C-homopolymer, where C interacts favorably with B. They focus on the situation where $\chi_{AB}N = 60$, $\chi_{AC}N = 60$, and $f_B = 0.2$. Here N is the diblock copolymer chain length and f_B its composition. Hence, the pure diblock copolymer system self-assembles into a bcc structure. Flat A/B interfaces are considered for $\chi_{BC} = 0$ only. Swollen micelles are obtained for homopolymer C solubilized in the spherical AB copolymer micelles also considering $\chi_{BC} < 0$. Their set of self-consistent-field equations can be used to address the problem considered in the present paper using strong segregation theory; however, the authors real interest concerned the encapsulation of nanoparticles in the center of the swollen micelles in the case of attraction between the surface of the particles and homopolymer C. Finally, in ref 30 ternary phase diagrams of A and B homopolymers with AC diblock copolymers are constructed, including the case where $\chi_{BC} < 0$.

As mentioned above, our interest here concerns the introduction of entanglements in self-assembled block copolymer systems by incorporating suitable homopolymers inside one of the block copolymer domains. Hence, we are particularly interested in how much homopolymer may be incorporated and its distribution. We limit ourselves to lamellar self-assembled

* Corresponding author. E-mail: g.ten.brinke@rug.nl.
[†] University of Groningen.
[‡] Russian Academy of Sciences.

10.1021/ma062527n CCC: $37.00
Published on Web 03/24/2007

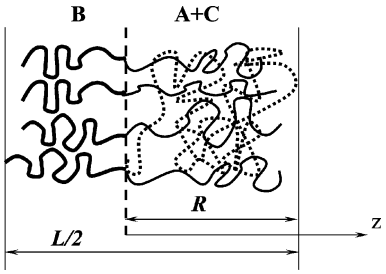

Figure 1. Schematic presentation of AB diblock copolymer/C homopolymer blend. The homopolymer chains segregate exclusively into A lamellar domains. A chains and B chains are depicted by thin and thick solid lines, respectively. Homopolymer chain is depicted by short-dashed lines. *R* is the thickness of half of the A layer, i.e., the distance from the interface to the mid-plane.

blends of a AB diblock copolymer with a homopolymer C that interacts favorably with the A blocks. All other interactions are assumed to be strongly unfavorable so that a strong segregation-type analysis is appropriate. Of course, the lamellar morphology is destroyed once the average volume fraction of homopolymer inside the lamellar domains is too large, and transitions to other morphologies will occur.[12] However, these are outside the scope of the present paper.

In the next sections the theoretical model will be introduced, and it will be shown how the pertinent parameters, such as amount of homopolymer added, interaction strength, block copolymer composition, etc., affect the distribution of the homopolymer inside the block copolymer A layer.

2. Theory

We consider a blend of a diblock copolymer AB and a homopolymer C, assuming from the very beginning that the homopolymer chain length N_C is longer than the total diblock copolymer length N. Each block copolymer chain consists of $N = N_A + N_B$ monomer units. The volume of the different monomers is assumed to be equal and is denoted by v. We also assume that the statistical segment length a of the A, B, and C molecules is the same. The ratio $f = N_A/N$ defines the diblock copolymer composition, and the ratio $\varphi = V_C/V_{total}$ represents the average homopolymer volume fraction in the mixture, V_C being the volume occupied by homopolymer and V_{total} the volume of the mixture. The Flory−Huggins interaction parameters χ_{AB} and χ_{BC} are taken to be positive, whereas the Flory−Huggins parameter χ_{AC} is supposed to be negative implying favorable interactions between homopolymer C and the A block of the diblock copolymer. The blend of polystyrene-*block*-poly(4-vinylpyridine) (PS-*b*-P4VP) and poly(2,6-dimethyl-1,4-diphenyl oxide) (PPO), where $\chi_{PS-PPO} = -0.1$,[31−33] $\chi_{PS-P4VP} = 0.3-0.35$,[34] and $\chi_{P4VP-PPO} \cong 0.6$,[35] serves as an experimental example and in fact motivated the present study.

In the strong segregation limit the A and B blocks are stretched and directed perpendicular to the narrow AB interface.[36] At this level of segregation we can model a diblock copolymer as a polymer brush. Considering exclusively the lamellar morphology, as we will do in this paper, each lamellar domain will consist of opposite brushes.[37] Since the B−C interactions are unfavorable ($\chi_{BC} > 0$), homopolymer C will segregate exclusively in the A domains, generally resulting in some nonuniform homopolymer distribution $\Phi(z)$ across the A lamellar domain (z is the coordinate perpendicular to the AB interface). A schematic illustration of the model considered is given in Figure 1. A somewhat similar situation also involving three components was considered in ref 38. There the situation was considered where nanoparticles are preferably distributed in one of the lamellar domains of a diblock copolymer. Assuming from the outset a homogeneous distribution of the nanoparticles, the authors derived an expression for the increase in lamellar period as a function of the nanoparticle volume fraction. Our main goal is to go beyond this approach by investigating the homopolymer distribution inside the A layers and to determine the maximum amount of homopolymer that can be dissolved in the A layers. To achieve these objectives, we need to obtain an expression for the free energy of the system in terms of the homopolymer distribution profile $\Phi(z)$ inside the A layers. Hence, in contrast to ref 38, we will assume a free chain ends distribution,[37,39−41] which results in an inhomogeneous homopolymer distribution. The fact that the free chain ends of the A chains are distributed nonuniformly indicates that in some cases the homopolymer may not even penetrate up to the very AB interface, but only up to a certain penetration depth. Therefore, two different regimes will be distinguished from the beginning. In the first regime the homopolymer is distributed throughout the whole layer, whereas in the second regime the homopolymer does not go all the way to the AB interface.

Let us start with the first regime. In this case the average homopolymer volume fraction ϕ in the A layers is defined by

$$\phi = \frac{1}{R}\int_0^R \Phi(z)\, dz \tag{1}$$

Here the equilibrium A block layer thickness R should be determined for a given homopolymer distribution from the minimization of the total free energy of the whole system. Note that from geometrical considerations the average homopolymer volume fraction ϕ in the A layers and the average homopolymer volume fraction $\varphi = V_C/V_{total}$ in the whole diblock copolymer system are related via the diblock composition f:

$$\phi = \frac{\varphi}{\varphi + f(1-\varphi)} \tag{2}$$

The total free energy per block copolymer chain as a function of the homopolymer distribution profile consists of the free energy of the AB interface, the elastic free energy due to the stretching of the copolymer blocks, and the interaction energy between the homopolymer and the A blocks:

$$F_1 = \gamma\Sigma + \frac{\pi^2 N v^2 (1-f)}{8a^2\Sigma^2} + \frac{3\pi^2\Sigma}{8a^2N^2f^2v}\int_0^R z^2(1-\Phi(z))\, dz - \frac{|\chi|\Sigma}{v}\int_0^R \Phi(z)(1-\Phi(z))\, dz \tag{3}$$

Here the free energy is given in kT energetic units. Σ is the interfacial area per block copolymer chain, $\chi_{AC} \equiv \chi$, and $\gamma = a\sqrt{\chi_{AB}}/v\sqrt{6}$ is the AB interface tension. The first term in expression 3 is the interfacial free energy. Note that in our treatment we restrict ourselves to the situation when $\gamma_{AB} \cong \gamma_{BC} \equiv \gamma$. In the case of $\gamma_{AB} \neq \gamma_{BC}$ the interfacial tension γ will depend on the concentration of homopolymer at the AB interface and therefore should be found self-consistently. The elastic free energy is represented as a sum of two contributions representing the chain elongation in the B and A lamellar domains (second and third term in (3), respectively). The third term in eq 3 represents the nonuniform chain stretching and therefore inhomogeneous distribution of the free ends of the A chains.[41] In fact, $1 - \Phi(z) = \Phi_A(z)$ determines this distribution. The last term in expression 3 takes into account the interactions between

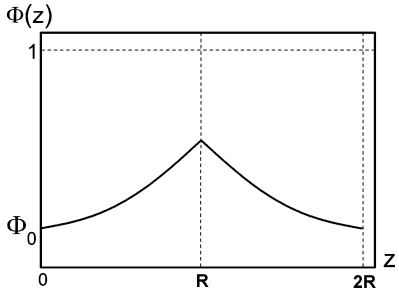

Figure 2. Schematic representation of typical parabolic concentration profile $\Phi(z) = \Phi_0 + \alpha z^2$, $\Phi_0 = \Phi_0(R,\Sigma)$, and $\alpha = \alpha(\chi)$.

the homopolymer C and the A blocks. Two more terms, which can be considered as corrections to the free energy, are omitted in expression 3. The first one is connected with the loss of conformational entropy of homopolymer C due to its nonuniform distribution inside the A layers. This term does become important for small values of interaction parameter $|\chi|$, and the case where this term dominates will be discussed later (section 3.1). We also omit the ideal-gas term which is connected with the thermal motion of the homopolymer and which scales as $1/N_C$.

To obtain an analytic expression for the homopolymer distribution $\Phi(z)$, the free energy (3) should be minimized under the constraint (1). Implementation of this procedure by the Lagrange multipliers method immediately results in a parabolic form for the homopolymer concentration profile (Figure 2):

$$\Phi(z) = \Phi_0 + \alpha z^2 \tag{4}$$

with

$$\Phi_0 = 1 - \frac{\alpha R^2}{3} - \frac{fN\upsilon}{\Sigma R} \tag{5}$$

$$\alpha = \frac{3\pi^2}{16a^2f^2N^2|\chi|}, \quad \Sigma R = \frac{fN\upsilon}{1-\phi} \tag{6}$$

Thus, the addition of some amount of homopolymer to the diblock copolymer results in a homopolymer distribution (4) inside the A layers. Distribution (4) shows a minimal amount of homopolymer, Φ_0, at interface where $z = 0$ and a maximum in the center of the lamellar domain, the so-called mid-plane, where $z = R$. Note that the inclusion of conformational effects will smoothen this profile in the center of the lamellar domain. Rewriting expression 4 in the form

$$\Phi(z) = \alpha(r^2 + z^2) \tag{7}$$

and introducing the dimensionless variable $u = R/r$, we can express r and R in terms of u:

$$r = \left[\frac{3\phi}{\alpha(u^3+3)}\right]^{1/2}, \quad R = \left[\frac{3\phi u^2}{\alpha(u^3+3)}\right]^{1/2} \tag{8}$$

It results in the following expression for the free energy:

$$F_1 = \gamma\Sigma + \frac{\pi^2 N\upsilon^2(1-f)}{8a^2\Sigma^2} + \frac{|\chi|\Sigma}{\upsilon}\left\{\alpha r^3\left[\frac{u^3}{3} - u\right] - \alpha^2 r^5\left[\frac{u^5}{5} - u\right]\right\} \tag{9}$$

Taking into account that $\Sigma R(1-\phi) = fN\upsilon$ and introducing a new parameter

$$k = \frac{\pi\gamma\upsilon}{4aN|\chi|^{3/2}} \tag{10}$$

which is a combination of all the different parameters occurring in the last expression for the free energy except for the diblock composition f, the final expression for the free energy is obtained in the form

$$\frac{F_1}{F_d} = \frac{(2k)^{1/3}}{3}\frac{\phi}{1-\phi}\left\{\frac{1}{\phi^{3/2}}\left[\frac{u^2+3}{u^2}\right]^{1/2} + \frac{1}{k}\left[2(1-f)(1-\phi)^3\frac{u^2}{u^2+3} + f\frac{u^2-3}{u^2+3} - \frac{9f\phi}{5}\frac{u^4-5}{(u^2+3)^2}\right]\right\} \tag{11}$$

Here $F_d = (3/2)(\pi\gamma\upsilon/2a)^{2/3}N^{1/3}$ is the free energy of the pure diblock copolymer system. As stated in the beginning, expression 11 is valid only as long as the homopolymer distribution continues up to the AB interface.

Now we turn our attention to the second regime assuming that this no longer holds. This regime appears for $\Phi_0 < 0$ (cf. eq 4). Physically, it implies the presence of a "dead zone", i.e., a region near the AB interface inside the A layer where the homopolymer does not penetrate (Figure 3). The average amount of homopolymer in the diblock copolymer/homopolymer system now satisfies

$$\phi = \frac{1}{R}\int_{R^*}^{R}\Phi(z)\,dz \tag{12}$$

Increasing the average amount of homopolymer added, the "dead zone" becomes smaller, and for some specific value of the average homopolymer concentration it will disappear. The condition $R^* = 0$ guarantees that the necessary amount of homopolymer has been added; after that Φ_0 starts to become positive.

Taking into account that the homopolymer is distributed only inside the interval $[R^*,R]$, the free energy given by eq 3 transforms into

$$F_2 = \gamma\Sigma + \frac{\pi^2 N\upsilon^2(1-f)}{8a^2\Sigma^2} + \frac{3\pi^2\Sigma}{8a^2N^2f^2\upsilon}\int_0^{R^*}z^2\,dz + \frac{3\pi^2\Sigma}{8a^2N^2f^2\upsilon}\int_{R^*}^{R}z^2(1-\Phi(z))\,dz - \frac{|\chi|\Sigma}{\upsilon}\int_{R^*}^{R}\Phi(z)(1-\Phi(z))\,dz \tag{13}$$

Minimization of the free energy (13) with respect to $\Phi(z)$ yields again a parabolic form for the homopolymer distribution profile. This profile satisfies the requirement $\Phi(R^*) = 0$ and reads

$$\Phi(z) = \alpha(z^2 - R^{*2}) \tag{14}$$

with constant α determined according to eq 6.

At this point we introduce a new variable $u = R/R^*$. Combining the homopolymer distribution profile (14) with condition (12) leads to the following expression for R and R^*, similar to (8):

$$R = \left[\frac{3\phi u^3}{\alpha(u^3-3u+2)}\right]^{1/2}, \quad R^* = \left[\frac{3\phi u}{\alpha(u^3-3u+2)}\right]^{1/2} \tag{15}$$

In terms of u the following expression for the free energy is obtained:

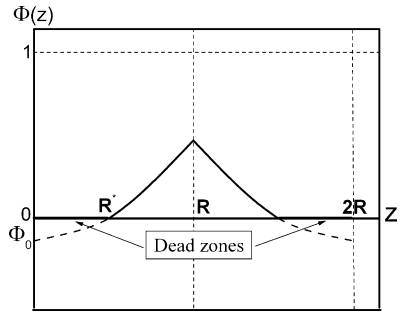

Figure 3. Schematic representation of typical parabolic concentration profile $\Phi(z) = \Phi_0 + \alpha z^2$ in the case when $\Phi(z = 0) = \Phi_0 < 0$.

$$F_2 = \gamma\Sigma + \frac{\pi^2 N v^2 (1-f)}{8a^2\Sigma^2} + \frac{|\chi|\Sigma}{v}\left\{\alpha R^{*3}\left[\frac{u^3}{3} + u - \frac{2}{3}\right] - \alpha^2 R^{*5}\left[\frac{u^5}{5} - u + \frac{4}{5}\right]\right\} \quad (16)$$

Applying the same sequence of calculations as described above, the free energy is found in the form

$$\frac{F_2}{F_d} = \frac{(2k)^{1/3}}{3}\frac{\phi}{1-\phi}\left\{\frac{1}{\phi^{3/2}}\left[\frac{u^3 - 3u + 2}{u^3}\right]^{1/2} + \frac{1}{k}\left[2(1-f)(1-\phi)^3\frac{u^3}{u^3 - 3u + 2} + f\frac{u^3 + 3u - 2}{u^3 - 3u + 2} - \frac{9f\phi}{5}\frac{u^6 - 5u^2 + 4u}{(u^3 - 3u + 2)^2}\right]\right\} \quad (17)$$

When the condition $R^* = 0$ is fulfilled, the second regime crosses over into the first one. For fixed values of f and k the free energies (11) and (17) are functions of the average homopolymer volume fraction ϕ and the dimensionless variable u. To see how the free energy behaves as a function of the homopolymer volume fraction, the free energy has to be minimized with respect to u. It is important to note that since we have a nonuniform distribution $\Phi(z)$, in contrast to the Alexander−de Gennes approach where the homopolymer is distributed uniformly, the maximum amount of homopolymer inside the lamellar domains is not determined by the location of the minimum of the free energy alone, as is shown in the Appendix for a Alexander−de Gennes brush, but involves in addition the requirement $\Phi(R) \leq 1$. This demand guarantees that the amount of homopolymer does not exceed unity in the center of the A domains, i.e., in the position where the homopolymer distribution has its maximum value.

3. Results and Discussion

The equations presented are used to numerically analyze different situations. First, the free energy is considered for a symmetric diblock copolymer for different values of $k = 0.2$, 0.5, and 0.8 and for different diblock copolymer compositions $f = 0.3$, 0.5, and 0.6 at fixed $k = 0.2$. The results are presented in Figures 4 and 5.

As shown in Figure 4 for a given diblock copolymer composition, the free energy is a decreasing function of the homopolymer volume fraction. This demonstrates that the penetration of the homopolymer is a favorable process up to a maximum concentration of homopolymer ϕ_{max} . ϕ_{max} is determined by the requirement $\Phi(R) \leq 1$. The maximum amount of homopolymer strongly depends on the value of the parameter $k = \pi\gamma v/(4aN|\chi|^{3/2})$. The larger k is, the smaller the maximum amount of homopolymer is. Small values of k correspond either

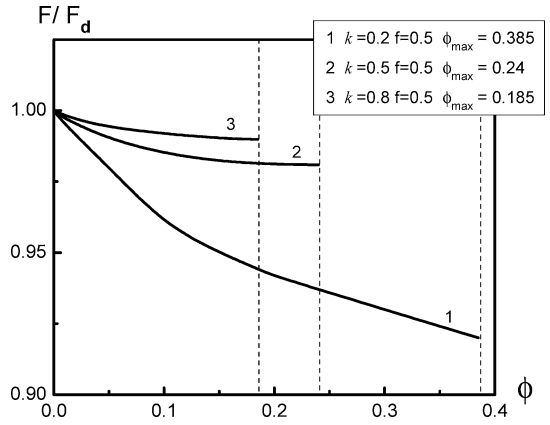

Figure 4. Numerically calculated free energies for different values of parameter k. Diblock copolymer composition $f = 0.5$. Dashed lines correspond to maximum allowable amount of homopolymer ϕ_{max} for values of k as indicated.

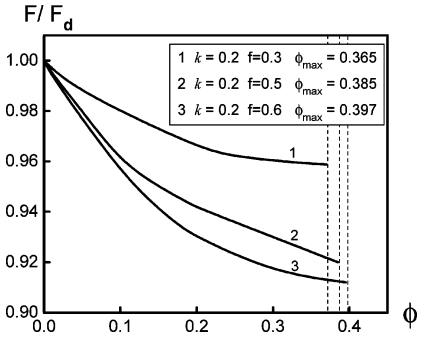

Figure 5. Numerically calculated free energies for different diblock compositions at $k = 0.2$. Dashed lines indicate maximum amount of homopolymer that can be dissolved for values of the diblock composition f as indicated.

to large values of N at fixed Flory−Huggins interaction parameter $|\chi|$ or to large values of $|\chi|$ at fixed diblock copolymer length N. The first statement shows that thicker lamellar domains can incorporate more homopolymer. The second observation implies that more favorable interactions, as expected, also allow more homopolymer to be dissolved. The analysis of Figure 5 shows that changes in diblock copolymer composition also affect the maximum possible amount of homopolymer inside the lamellar domains: the larger the volume fraction of A blocks in the diblock copolymer, the larger the amount of homopolymer that can be incorporated. A comparison between Figures 4 and 5 reveals that the maximum allowable homopolymer amount ϕ_{max} is, however, much more sensitive to changes in k than to changes in the diblock copolymer composition.

As already mentioned, the maximum allowable homopolymer amount ϕ_{max} also depends on the diblock copolymer chain length N. The numerically obtained dependence is depicted in Figure 6 for a symmetric diblock copolymer taking $\chi_{AB} = 0.32$. For extremely small values of k, which is the case for very strong favorable AC interactions or very long diblock copolymers, the maximum value of ϕ_{max} approaches unity. Referring to the experimental example already introduced before, in the case of a P4VP−PS/PPO blends with $\chi_{PS-PPO} = -0.1$, $\chi_{PS-P4VP} = 0.32$, and a number of monomer units $N = 1000$, we have $k = 0.006$, implying $\phi_{max} = 0.82$. Experimentally, it has indeed been observed that PPO homopolymer can be incorporated in PS domains up to a large amount. However, as mentioned before, for large amounts of homopolymer the lamellar structure will obviously no longer correspond to the equilibrium morphology.

The presence of "dead zones" is illustrated by the behavior of R^*/R as a function of average homopolymer concentration ϕ

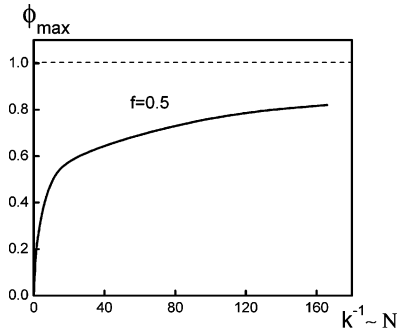

Figure 6. Maximum allowable amount of homopolymer as a function of diblock chain length *N*. For infinitely long diblock copolymer chains ϕ_{max} asymptotically approaches unity.

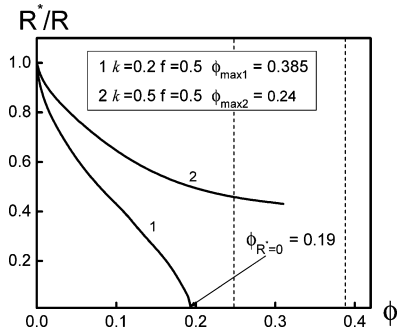

Figure 7. Dependence of homopolymer penetration depth on average homopolymer volume fraction for different values of parameter *k*. The figure represents two different situations corresponding to the presence (curve 1) and absence (curve 2) of homopolymer at the AB interface. Dashed lines depict maximum allowable average homopolymer concentrations for indicated values of *k*.

presented in Figure 7 for two different situations. Curve 1 in this figure corresponds to the case $k = 0.2$ and demonstrates that for an average homopolymer concentration $\phi = 0.19$ switching between the two regimes occurs; i.e., at $\phi = 0.19$ the condition $R^* = 0$ is fulfilled. This means that at $k = 0.2$ for all average homopolymer concentrations satisfying $\phi > 0.19$ we will always have some amount of homopolymer at the AB interface. The maximum amount of homopolymer in the A layers equals $\phi_{max\,1} = 0.385$. Curve 2 in Figure 7 for $k = 0.5$ with $\phi_{max\,2} = 0.24$ represents the opposite situation where we will never have homopolymer present at the AB interface; in this case R^* is never zero. It happens because the average homopolymer concentration achieves it maximum allowable value $\phi_{max\,2} = 0.24$ before the switching between the two regimes takes place. In the case depicted by curve 2 in Figure 7 the system will always remain in the second regime, whereas for the situation represented by curve 1 in Figure 7 there is a crossover between the two regimes.

Homopolymer distribution profiles for $k = 0.006$ and for different average homopolymer volume fractions are presented in Figure 8a−c. The value $k = 0.006$ corresponds to P4VP-*b*-PS/PPO blend with $f = 0.5$, $\chi_{PS-PPO} = -0.1$, $\chi_{PS-P4VP} = 0.32$, and number of monomer units $N = 1000$. Our approach therefore predicts that starting from a volume fraction $\phi_{PPO} = 0.013$ PPO will go up to the PS/P4VP interface.

Next we consider how the lamellar period changes in the presence of the homopolymer. Without the homopolymer the long period *L* of pure diblock copolymers reads[36]

$$L_d = \left(\frac{2aN}{\pi}\right)^{2/3} (\gamma v)^{1/3} \qquad (18)$$

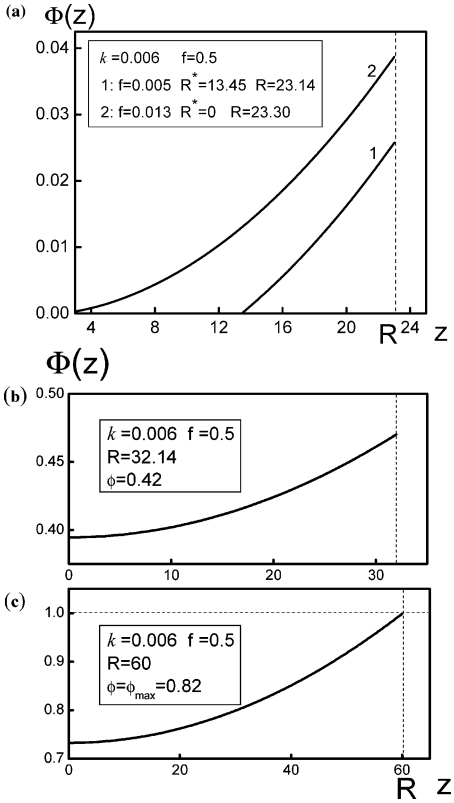

Figure 8. Calculated homopolymer concentration profiles for different average homopolymer volume fractions ϕ for $k = 0.006$, with a maximum possible average amount of homopolymer $\phi_{max} = 0.82$. (a) Curve 1: the absence of homopolymer at the AB interface is illustrated for $\phi = 0.005$. Ratio $R^*/R = 0.58$. Curve 2: average homopolymer volume fraction is increased up to $\phi = 0.013$. Here the homopolymer goes very close to the AB interface and is distributed through the A domains with a parabolic distribution profile. (b) Homopolymer distribution for an intermediate value of the average concentration of homopolymer, $\phi = 0.42$, with the minimum homopolymer fraction at the interface ($z = 0$) and the maximum in the center of A lamellar domain ($z = R$). (c) Homopolymer distribution for $\phi = \phi_{max} = 0.82$. In the center of the A layers $\Phi(R) = 1$, indicating that more homopolymer cannot be incorporated.

The long period *L* of the copolymer/homopolymer blend is directly related to the thickness of the A layers. This in turn depends on the average homopolymer concentration as determined by the minimization of the free energy given by eq 11 or eq 17. In the first regime (expression 11 for the free energy is used) the behavior of the long period *L* as a function of average homopolymer volume fraction ϕ is found to be given by the expression

$$\frac{L}{L_d} = \left(\frac{4}{k}\right)^{1/3} \phi^{1/2}(1 - \phi(1 - f))\left[\frac{u^2}{u^2 + 3}\right]^{1/2} \qquad (19)$$

In the second regime where the free energy is given by eq 17 the long period *L* satisfies

$$\frac{L}{L_d} = \left(\frac{4}{k}\right)^{1/3} \phi^{1/2}(1 - \phi(1 - f))\left[\frac{u^3}{u^3 - 3u + 2}\right]^{1/2} \qquad (20)$$

In these equations *u* has a value which is determined by minimization of eqs 11 and 17. The combination of expressions 19 and 20 gives the long period of the diblock copolymer/homopolymer blend for all homopolymer volume fractions that are allowed. Subsequent numerical calculations showed the change in the lamellar period in the presence of homopolymer (Figure 9a). The situation depicted by curve 3 in this figure

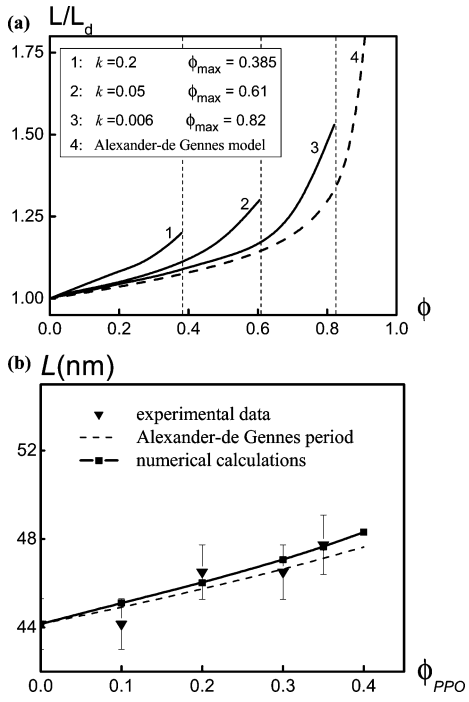

Figure 9. Top: changes in period L in the presence of homopolymer are depicted for symmetric diblock for different values of k. Dashed line shows long period predicted by the Alexander−de Gennes approach. Bottom: comparison of the results of numerical calculations and experimental data for $f = 0.5$, $\chi_{AB} = 0.32$, and $N = 400$ ($k = 0.014$).

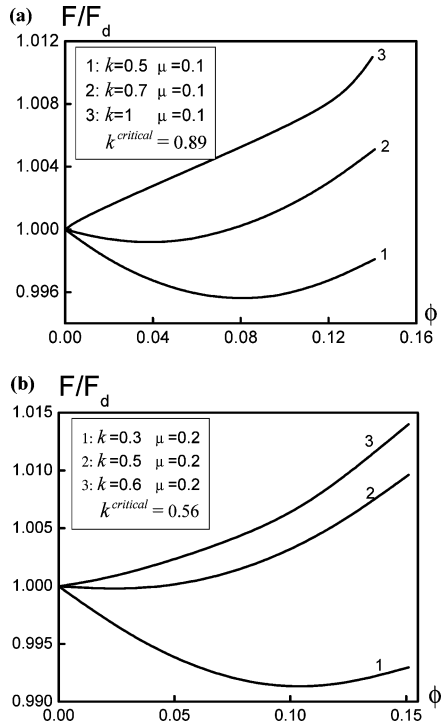

Figure 10. Free energy as a function of average homopolymer volume fraction for different values of parameters k and μ. Top: $\mu = 0.1$, $k = 0.5$, 0.7, 1.0. For $k > k^{\text{critical}} = 0.89$ the free energy is an increasing function of the average homopolymer volume fraction; bottom: $\mu = 0.2$, $k = 0.3$, 0.5, 0.6, $k^{\text{critical}} = 0.56$.

corresponds to the familiar experimental example of P4VP−PS/PPO with $k = 0.006$. In all cases the long period L increases as a function of the amount of homopolymer inside the lamellar domains. Figure 9b compares the results of the numerical calculations with the experimental data for the P4VP−PS/PPO blend. The parameter values for the numerical calculations were taken from the experiments in ref 22: $f = 0.5$, $\chi_{AB} = \chi_{PS-P4VP} = 0.32$, and $N = N_{PS-P4VP} = 400$. The dashed line in Figure 9a represents the behavior of the long period as predicted by the Alexander−de Gennes model, assuming that all chain ends are at the mid-plane and that the homopolymer is distributed uniformly throughout the layer. As one can see, curve 4 in Figure 9a demonstrates that for small values of k (large ϕ_{max}) the long period L asymptotically approaches the Alexander−de Gennes prediction. This is evidence that for large values of the diblock copolymer length N and Flory−Huggins parameter $|\chi_{AC}|$ the Alexander−de Gennes model can be considered as a limiting case of our more general model with nonuniform homopolymer distribution. Note that in the case of the Alexander−de Gennes approach, due to the uniform homopolymer distribution ratio, L/L_d is independent of k and is given by (see also ref 38)

$$\frac{L}{L_d} = \left(1 + \frac{f\phi}{1-\phi}\right)\left(1 - f + \frac{f}{(1-\phi)^2}\right)^{1/3} \tag{21}$$

whereas in our case because of the inhomogeneous distribution the ratio L/L_d depends on k as reflected in eqs 19 and 20. For the P4VP-*b*-PS/PPO blends the difference in long period between our more elaborated model and the simplified Alexander−de Gennes picture is relatively small, and both descriptions describe the experimental data within experimental errors (Figure 9b).

3.1. Conformational Effects. So far the conformational effects due to the inhomogeneous distribution of the homopolymer have been neglected. These start to become important if the interaction parameter $|\chi|$ is small. By substitution of the analytic expressions for the homopolymer distribution profiles presented in Figure 8b,c into expression 3 for the free energy, we can verify that the conformational term[36]

$$F_{\text{conform}} = \frac{a^2\Sigma}{24\upsilon}\int_0^R \frac{[\nabla\Phi(z)]^2\,dz}{\Phi(z)(1-\Phi(z))} \tag{22}$$

is actually small compared to the other terms in expression 3. It turns out that for the situation depicted in Figure 8a, where the average homopolymer concentration is small, this is no longer the case. This forces us to consider in more detail the conformational free energy contribution for small average homopolymer volume fractions. Taking into account the loss of conformational entropy, the free energy (1) reads

$$F = \gamma\Sigma + \frac{\pi^2 N\upsilon^2(1-f)}{8a^2\Sigma^2} + \frac{3\pi^2\Sigma}{8a^2N^2f^2\upsilon}\int_0^R z^2(1-\Phi(z))\,dz - \frac{|\chi|\Sigma}{\upsilon}\int_0^R \Phi(z)(1-\Phi(z))\,dz + \frac{a^2\Sigma}{24\upsilon}\int_0^R \frac{[\nabla\Phi(z)]^2\,dz}{\Phi(z)(1-\Phi(z))} \tag{23}$$

Again, to get the homopolymer distribution profile the free energy (23) should be minimized with respect to $\Phi(z)$. In order to simplify our calculations, we use the function

$$\Phi(x) = \frac{\Phi_0}{ch^2\alpha x} \tag{24}$$

as a trial function for the homopolymer distribution profile. The particular feature of this function is that it makes the homopolymer distribution profile smoother compared to a parabolic profile, and thus the homopolymer distribution has no longer a

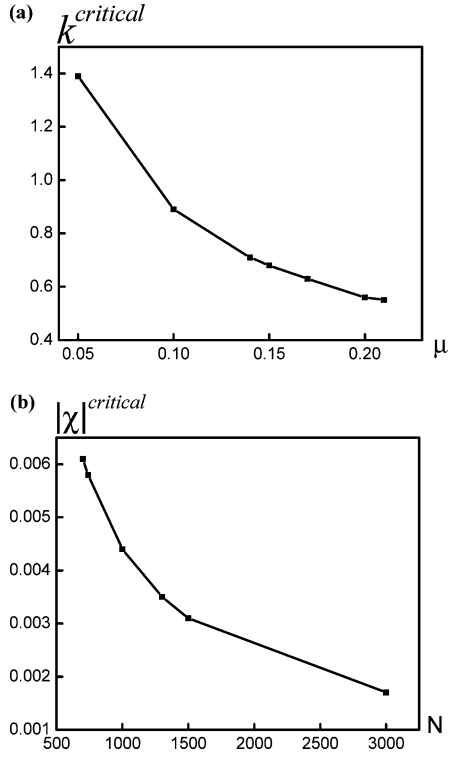

Figure 11. Numerically calculated dependences: (top) $k^{\text{critical}} = k^{\text{critical}}(\mu)$; (bottom) $|\chi|^{\text{critical}} = |\chi|^{\text{critical}}(N)$ at fixed $\chi_{AB} = 0.32$.

sharp break in the center of the lamellar domain. The result of substitution of (24) into (23) is straightforward and brings us to the expression for the free energy in terms of $\tilde{x} = R/R_d$, where $R_d = f(2aN/\pi)^{2/3}(\gamma v)^{1/3}$ is the period of the pure diblock copolymer and $\Phi_0 = \alpha R\phi$ is determined from eq 1 for the homopolymer distribution profile (24). Hence, including the conformational term the free energy becomes

$$\frac{F}{F_d} = \frac{1}{1-\phi}\left\{\frac{2}{3\tilde{x}} + f\tilde{x}^2\left[\frac{(1-f)(1-\phi)^3}{3f} + \frac{1}{3} - \phi + \frac{2\phi^2 \ln 2}{\Phi_0}\right] - \frac{2f\phi}{3(2k)^{2/3}}\left[1 - \frac{2}{3}\Phi_0\right] + \frac{2\Phi_0\mu^{4/3}}{9\phi f\tilde{x}^2}\left[1 - \sqrt{\frac{1-\Phi_0}{\Phi_0}}\arctan\sqrt{\frac{\Phi_0}{1-\Phi_0}}\right]\right\} \quad (25)$$

In eq 25 k has been introduced by (10), and $F_d = (3/2)(\pi\gamma v/2a)^{2/3}N^{1/3}$ is the free energy of the pure diblock copolymer. Compared to eq 11 or 17, we have one more parameter

$$\mu = \sqrt{\frac{\pi}{2N}}\frac{a}{v\gamma} = \sqrt{\frac{3\pi}{\chi_{AB}N}} \quad (26)$$

which does not depend on homopolymer properties and is determined only by the diblock copolymer, its length N, and the Flory−Huggins parameter χ_{AB}.

Subsequently, the free energy (25) was minimized numerically with respect to $\tilde{x}$ and Φ_0. But before presenting the results, we first discuss the qualitative changes that may be anticipated from conformational effects. When these effects were not considered the free energy behaved as a decreasing function of the average homopolymer volume fraction for arbitrary negative values of the Flory−Huggins interaction parameter $\chi_{AC} \equiv \chi$ (see for example Figure 4). It implied that the penetration of homopolymer into A lamellar domains is favorable even for very weakly attractive AC interactions, i.e., even for very small

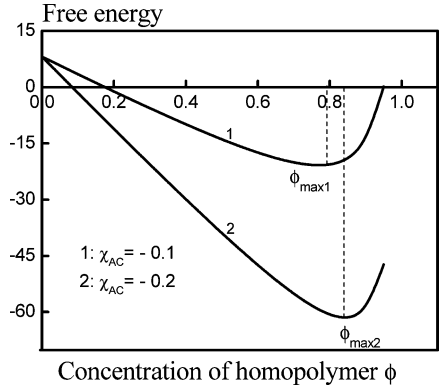

Figure 12. Calculated free energy per block copolymer chain as a function of homopolymer concentration ϕ. $f = 0.5$, $\chi_{AB} = 0.32$, and $N = 1000$.

values of the Flory−Huggins interaction parameter $|\chi|$. Including conformational effects, in the case of weakly favorable AC interactions (which corresponds to the case where only a small amount of homopolymer can be incorporated in the lamellar structure) the entropic penalty due to the loss of conformational entropy becomes bigger compared to the strength of the weakly favorable interactions. Therefore, in this case the conformational effects play a determining role.[42] Consequently, there should exist a critical value $|\chi|^{\text{critical}}$ such that for all $|\chi| \le |\chi|^{\text{critical}}$ penetration of homopolymer is no longer favorable. Referring to eq 10, this means that there is some critical value k^{critical} such that for all $k \ge k^{\text{critical}}$ penetration of homopolymer is unfavorable. These qualitative considerations are confirmed by the results of the numerical calculations shown in Figure 10a,b. As follows from the numerical calculations for $\mu = 0.1$, there is a critical value $k^{\text{critical}} = 0.89$ such that for $k < k^{\text{critical}}$ the free energy reaches a minimum as a function of the average amount of homopolymer (see Figure 10a). The position of this minimum defines the maximum amount of homopolymer able to penetrate inside the lamellar domain for given value of μ. It follows from eq 26 that the value of μ is determined by the diblock length N and the interaction parameter χ_{AB}. If the latter is constant, μ depends only on the diblock copolymer length N. Since longer diblock copolymers can incorporate more homopolymer and because μ scales as $N^{-1/2}$, one can conclude that for smaller values of μ more homopolymer can be incorporated for the same value of parameter k. This conclusion is corroborated by numerical calculations presented in Figure 10. The minimum in curve 1 in Figure 10a for $k = 0.5$, $\mu = 0.1$ is shifted to the right compared to the position of the minimum in curve 2 in Figure 10b for $k = 0.5$, $\mu = 0.2$. In other words, the minimum for $k = 0.5$, $\mu = 0.1$ corresponds to a larger amount of homopolymer in comparison with $k = 0.5$, $\mu = 0.2$. In the case where μ is constant, increasing the Flory−Huggins parameter value $|\chi|$ decreases the value of k, making it smaller than k^{critical}. This allows to incorporate more homopolymer inside lamellar domain, as demonstrated by Figure 10a,b.

A comparison of eqs 10 and 26 yields the following expressions for $|\chi|N$:

$$|\chi|N = \frac{\pi}{2(2k\mu)^{2/3}} \quad (27)$$

The numerical calculations show that k^{critical} and $|\chi|^{\text{critical}}$ behave as a function of μ and diblock copolymer chain length N, as presented in parts a and b of Figure 11, respectively. Here, the Flory−Huggins interaction parameter χ_{AB} was taken to be 0.32. For a diblock copolymer length $N = 1000$ and $\chi_{AB} = 0.32$, the

critical value $k^{\text{critical}} = 0.63$, and therefore according to eq 10 $|\chi|^{\text{critical}} = 0.0044$. Hence, for all $|\chi| < |\chi|^{\text{critical}} = 0.0044$ penetration of homopolymer will not be favorable.

4. Conclusions

In this paper, we presented a theoretical analysis of the lamellar self-assembled state of blends of a diblock copolymer and a long homopolymer where the homopolymer is assumed to interact favorably with one of the blocks of the diblock copolymer. Throughout the discussion a strong segregated lamellar morphology is assumed to be present with the homopolymer dissolving exclusively in one of the two different layers. The essential parameter governing the incorporation of the homopolymer inside the corresponding lamellar domains turned out to be $k = (\pi\gamma\upsilon)/(4aN|\chi|^{3/2})$. Here γ is the interfacial tension, N the block copolymer chain length, and χ the Flory−Huggins parameter representing the favorable interactions between the homopolymer and the corresponding block. The homopolymer is assumed to have a chain length exceeding N. Furthermore, γ is assumed to be constant even if some homopolymer is present at the interface.

The value of k determines whether the dissolved homopolymer will be able to reach the interface. If k is sufficiently small, this will be possible, however, for the homopolymer to be actually present at the interface the amount of homopolymer still has to exceed some critical average volume fraction. If that is the case, the homopolymer distribution is close to parabolic with its minimum at the interface and its maximum in the center of lamellar microdomain, i.e., at the mid-plane. If these requirements are not met, a "dead" zone will be present near the block copolymer interface where no homopolymer is present. Additionally, the maximal amount of homopolymer that can be incorporated may also be bounded. This property is, however, of less interest since for a large amount of homopolymer the assumption of the lamellar morphology will in general no longer hold.

These predictions are based on calculations that assume the homopolymer conformational effects due to the inhomogeneous distribution of homopolymer to be small. Such effects do, however, become important in the case of weakly favorable homopolymer−block copolymer interactions, i.e., $|\chi| \ll 1$. Since these conformational effects are unfavorable regarding the dissolution of the homopolymer into the lamellar domains, a critical value $|\chi|^{\text{critical}}$ exists such that for all $|\chi| \leq |\chi|^{\text{critical}}$ the homopolymer will not dissolve.

Acknowledgment. Financial support from Netherlands Organization for Scientific Research (NWO) within the Dutch-Russian scientific cooperation program is gratefully acknowledged. The Russian Foundation of Basic Research (RFBR) is also acknowledged (Grant 06-03-32641).

Appendix. Alexander−de Gennes Approach

In this appendix, we consider the so-called Alexander−de Gennes approximation: homopolymer C with average volume fraction ϕ is uniformly distributed throughout the A layers of lamellar self-assembled AB diblock copolymers. The diblock copolymer chain ends are considered to be fixed at the mid-plane. The set of Flory−Huggins interaction parameters satisfies the same conditions as before: $\chi_{AB} > 0$, $\chi_{BC} > 0$, and $\chi_{AC} < 0$. Because of the presence of component C in the A layer, the thickness of this part becomes

$$R_A = \frac{fN\upsilon}{(1-\phi)\Sigma} \tag{A1}$$

where symbols f, N, and υ denote the same physical quantities as before.

The thickness of the B layer is independent of concentration of homopolymer C and reads as follows:

$$R_B = \frac{(1-f)N\upsilon}{\Sigma} \tag{A2}$$

The free energy per block copolymer chain is given by

$$F = \gamma\Sigma + \frac{3R_A^{\,2}}{2fNa^2} + \frac{3R_B^{\,2}}{2(1-f)Na^2} + \chi fN\phi \tag{A3}$$

Substitution of eqs A1 and A2 into eq A3 yields the following expression:

$$F = \frac{3N\upsilon^2}{2\Sigma^2 a^2}\left((1-f) + \frac{f}{(1-\phi)^2}\right) + \gamma\Sigma + \chi fN\phi \tag{A4}$$

Subsequent minimization of eq A4 with respect to Σ, i.e. $dF/d\Sigma = 0$, leads to the final expression for free energy per block copolymer chain:

$$F = \frac{3}{2}\left[\frac{3N\upsilon^2\gamma^2}{a^2}\right]^{1/3}\left((1-f) + \frac{f}{(1-\phi)^2}\right)^{1/3} + \chi fN\phi \tag{A5}$$

For $f = 0.5$, $\chi_{AB} = 0.32$, and $N = 1000$, the free energy per block copolymer chain for different values of Flory−Huggins interaction parameter χ_{AC} behaves as a function of the average homopolymer concentration ϕ, as presented in Figure 12. For all homopolymer volume fractions $\phi < \phi_{max}$ it is energetically favorable to dissolve into the A block lamellar domains. For $\phi \geq \phi_{max}$ only an amount ϕ_{max} will dissolve into the A lamellar domains; the rest will macrophase separate. The more favorable the interactions between the homopolymer and the A blocks the larger the amount of homopolymer that can be incorporated in the A domains, provided, of course, the lamellar structure is present.

References and Notes

(1) Hamley, I. W. *The Physics of Block Copolymers*; Oxford University Press: Oxford, 1998.
(2) Hashimoto, T.; Tanaka, H.; Hasegawa, H. *Macromolecules* **1990**, *23*, 4378.
(3) Tanaka, H.; Hashimoto, T.; Hasegawa, H. *Macromolecules* **1991**, *24*, 240.
(4) Winey, K. I.; Thomas, E. L.; Fetters, L. J. *Macromolecules* **1991**, *24*, 6182.
(5) Shull, K.; Mayes, A. M.; Russell, T. P. *Macromolecules* **1993**, *26*, 3929.
(6) Mayes, A. M.; Russel, T. P.; Satija, S. K.; Majkrzak, C. F. *Macromolecules* **1992**, *25*, 6523.
(7) Shull, K. R.; Winey, K. I. *Macromolecules* **1992**, *25*, 2637.
(8) Kinning, D. J.; Thomas, E. L.; Fetters, L. J. *J. Chem. Phys.* **1989**, *90*, 5806.
(9) Winey, K. I.; Thomas, E. L.; Fetters. L. J. *J. Chem. Phys.* **1991**, *95*, 9367.
(10) Bodycomb, J.; Yamaguchi, D.; Hashimoto, T. *Macromolecules* **2000**, *33*, 5187.
(11) Lee, J. H.; Balsara, N. P.; Chakraborty, A. K.; Krishnamoorti, R.; Hammouda, B. *Macromolecules* **2002**, *35*, 7748.
(12) Semenov, A. N. *Macromolecules* **1993**, *26*, 2273.
(13) Likhtman, A. E.; Semenov, A. N. *Macromolecules* **1997**, *30*, 7273.
(14) Semenov, A. N. *Macromolecules* **1992**, *25*, 4967.
(15) Matsen, M. W. *Macromolecules* **1995**, *28*, 5765.
(16) Janert, P. K.; Schick, M. *Macromolecules* **1998**, *31*, 1109.
(17) Lee, H.-K.; Kang, C.-K.; Zin, W.-C. *Polymer* **1997**, *38*, 1595.

(18) Ahn, J.-H.; Sohn, B.-H.; Zin, W.-C.; Noh, S.-T. *Macromolecules* **2001**, *34*, 4459.
(19) Tucker, P. S.; Barlow, J. W.; Paul, D. R. *Macromolecules* **1988**, *21*, 1678.
(20) Tucker, P. S.; Barlow, J. W.; Paul, D. R. *Macromolecules* **1988**, *21*, 2794.
(21) Hashimoto, T.; Kimishima, K.; Hasegawa, H. *Macromolecules* **1991**, *24*, 5704.
(22) van Zoelen, W.; Alberda van Ekenstein, G. O. R.; Ikkala, O.; ten Brinke, G. *Macromolecules* **2006**, *39*, 6574.
(23) Olabisi, O.; Robeson, L. M.; Shaw, M. T. *Polymer-Polymer Miscibility*; Academic Press: New York, 1979.
(24) van Zoelen, W.; Alberda van Ekenstein, G. O. R.; Polushkin, E.; Ikkala, O.; ten Brinke, G. *Soft Matter* **2005**, *1*, 280.
(25) Borukhov, I.; Leibler, L. *Phys. Rev. E* **2000**, *62*, R41.
(26) Borukhov, I.; Leibler, L. *Macromolecules* **2002**, *35*, 5171.
(27) Lee, J. H.; Ruegg, M. L.; Balsara, N. P.; Zhu, Y.; Gido, S. P.; Krishnamoorti, R.; Kim, M.-H. *Macromolecules* **2003**, *36*, 6537.
(28) Ruegg, M. L.; Reynolds, B. J.; Lin, M. Y.; Lohse, D. J.; Balsara, N. P. *Macromolecules* **2006**, *39*, 1125.
(29) Lefebvre, M. D.; Shull, K. R. *Macromolecules* **2006**, *39*, 3450.
(30) Denesyuk, N. A.; Gompper, G. *Macromolecules* **2006**, *39*, 5497.
(31) Weeks, N. E.; Karasz, F. E.; MacKnight, W. J. *J. Appl. Phys.* **1977**, *48*, 4068.
(32) Kambour, R. P.; Bendler, J. T.; Bopp, R. C. *Macromolecules* **1983**, *16*, 753.
(33) ten Brinke, G.; Karasz, F. E.; MacKnight, W. J. *Macromolecules* **1983**, *16*, 1827.
(34) Alberda van Ekenstein, G. O. R.; Meyboom, R.; ten Brinke, G.; Ikkala, O. *Macromolecules* **2000**, *33*, 3752.
(35) de Wit, J.; Alberda van Ekenstein, G. O. R.; ten Brinke, G. *Polymer*, in press.
(36) Semenov, A. N. *Sov. Phys. JETP* **1985**, *61*, 733.
(37) Milner, S. T.; Witten, T. A.; Cates, M. E. *Macromolecules* **1988**, *21*, 2610.
(38) Hamdoun, B.; Ausserre, D.; Cabuil, V.; Joly, S. *J. Phys. II* **1996**, *6*, 503.
(39) Kim, J. U.; O'Shaughenessy, B. *Macromolecules* **2006**, *39*, 413.
(40) Witten, T. A.; Leibler, L.; Pincus, P. A. *Macromolecules* **1990**, *23*, 824.
(41) Subbotin, A.; de Jong, J.; ten Brinke, G. *Eur. Phys. J. E* **2006**, *20*, 99.
(42) Hasewaga, R.; Aoki, Y.; Doi, M. *Macromolecules* **1996**, *29*, 6656.

MA062527N